

See discussions, stats, and author profiles for this publication at: <https://www.researchgate.net/publication/6935215>

Effects of Simultaneously Doped and Deposited Ag on the Photocatalytic Activity and Surface States of TiO₂

ARTICLE *in* THE JOURNAL OF PHYSICAL CHEMISTRY B · MARCH 2005

Impact Factor: 3.3 · DOI: 10.1021/jp0469618 · Source: PubMed

CITATIONS

306

READS

192

5 AUTHORS, INCLUDING:



Baifu Xin

Heilongjiang University

7 PUBLICATIONS 540 CITATIONS

SEE PROFILE



Zhiyu Ren

Heilongjiang University

45 PUBLICATIONS 1,086 CITATIONS

SEE PROFILE



Baiqi Wang

Tianjin Medical University

13 PUBLICATIONS 710 CITATIONS

SEE PROFILE

Effects of Simultaneously Doped and Deposited Ag on the Photocatalytic Activity and Surface States of TiO₂

Baifu Xin, Liqiang Jing, Zhiyu Ren, Baiqi Wang, and Honggang Fu*

Laboratory of Physical Chemistry, School of Chemistry and Materials Science,
Heilongjiang University, Harbin 150080, China

Received: July 9, 2004; In Final Form: December 7, 2004

Ag–TiO₂ catalysts with different Ag contents were prepared via a sol–gel method in the absence of light. Based on the characterizations of XRD, photoluminescence (PL), surface photovoltage spectroscopy (SPS), field-induced surface photovoltage spectroscopy (FISPS), and XPS as well as the evaluation of the photocatalytic activity for degrading rhodamine B(RhB) solutions, it was found that the Ag dopant promoted the phase transformation as well as had an inhibition effect on the growth of anatase crystallite. The PL and SPS intensities were decreased with increasing Ag content, indicating that the Ag dopant could effectively inhibit the recombination of the photoinduced electrons and holes. However, the active sites capturing the photoinduced electrons reduced, while the Ag content exceeded 5 mol %. At rather low Ag dopant concentrations, the migration and diffusion of Ag⁺ ions were predominant, while at rather high Ag dopant concentrations, the migration, diffusion, and reduction of Ag ions simultaneously occurred. The Ag–TiO₂ photocatalysts with appropriate content of Ag (Ag species concentration is from about 3 to 5 mol %) possessed abundant electron traps so as to be favorable for the separation of the photoinduced electron–hole pairs, which could greatly enhance the activity of the photocatalysts. From the results of FISPS measurements, it could be found that the impurity bands and abundant surface states were introduced into the interfacial layer of TiO₂ because of Ag simultaneously doping and depositing, which could improve the absorption capability for visible light of the photocatalysts.

1. Introduction

Nanosized TiO₂, one of the most popular photocatalysts, has long been investigated for photocatalytic degradation of organic pollutants,¹ photocatalytic dissociation of water,² and solar energy conversion.³ However, the efficiency of photocatalytic reactions is limited by the high recombination rate of photoinduced electron–hole pairs formed in photocatalytic processes and by the absorption capability for visible light of photocatalysts. Many studies have been devoted to the improvement of photocatalytic activity of TiO₂ by depositing noble metals.^{4–11} The deposited metals on the surface of TiO₂ can produce traps to capture the photoinduced electrons or holes, leading to the reduction of electron–hole recombination in photocatalytic processes and the increase in the absorption capability for visible light of TiO₂ particles. However, some noble metals such as Pt, Pd, Rh, and Au are too expensive to be used in industrial scale. Thus, the research of Ag-modified TiO₂ has more significant practical value.

Ag–TiO₂ prepared by a photoreduction method has already been investigated by several research groups.^{7–10} It could be found that the photocatalytic activity of Ag–TiO₂ prepared by this method is unable to be improved obviously in comparison with that of pure TiO₂. The main reason for this fact is that photoreduced Ag cannot be highly dispersed on the surface of TiO₂, so that the amount of active sites on the Ag–TiO₂ surface cannot markedly increase, and the electronic structure of TiO₂ photocatalyst cannot change greatly. Moreover, the content of Ag deposited on the surface of TiO₂ cannot be effectively

controlled. To overcome these difficulties and disadvantages, we have developed a novel method to prepare the Ag-modified TiO₂. Ag–TiO₂ catalysts with different Ag/Ti molar ratios have been prepared by a sol–gel method in the absence of light, which would avoid Ag⁺ being photoreduced during the gel formation. A part of AgNO₃ was then thermal decomposed or reduced to metallic Ag, which can be deposited onto the surface of TiO₂; meanwhile, a small amount of Ag ions diffused into the lattice of TiO₂. This preparation method of the simultaneously doped and deposited Ag–TiO₂ catalyst has not been reported by other groups.

In this paper, the different Ag/Ti molar ratio Ag–TiO₂ nanoparticle photocatalysts are prepared. The prepared samples were characterized by XRD, XPS, SPS, and PL spectra. The effects of the simultaneously depositing and doping of Ag species on the surface states, surface energy levels, and interfacial electron transfer were investigated. In addition, the photocatalytic activity of the Ag–TiO₂ was evaluated.

2. Experimental Section

2.1. Preparation of Ag–TiO₂ Photocatalyst. A certain amount of AgNO₃ was dissolved in a mixture of 3 mL of ethanol and 2 mL of deionized water (solution A). Another mixture consisted of 7.6 mL of Ti(OBu)₄, 7 mL of ethanol, and 3 mL of N(C₂H₅OH)₃ (solution B). Solution A was then added dropwise to solution B under vigorously stirring in the dark, and the mixed solution was continuously stirred until the gel was formed. The gel was dried at 100 °C, calcined at 400 °C, and ground to obtain the Ag–TiO₂ nanoparticles. The Ag concentrations in the samples were 0, 0.01, 0.03, 0.05, 0.1, 0.3, 0.5, 1, 2, 3, 5, 7, and 10 mol %, respectively.

* Corresponding author. Tel.: 86-0451-86608458. Fax: 86-0451-86673647. E-mail: fuhg@vip.sina.com.

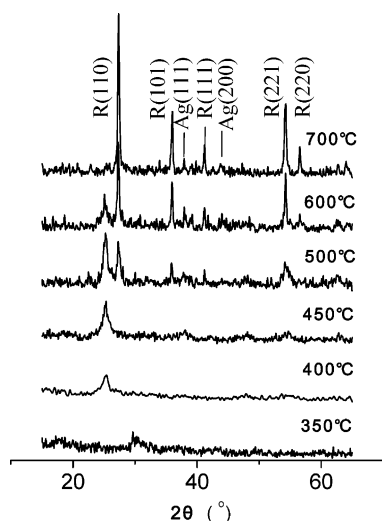


Figure 1. The XRD patterns of the 5 mol % Ag-TiO₂ calcined at different temperatures for 2 h.

2.2. Characterization of Samples. X-ray diffraction (XRD) analysis of TiO₂ powders was carried out on a Rigaku D/MAX-rA X-ray diffractometer, employing Cu K α (Ni filtered) radiation $\lambda = 0.15418$ nm. The patterns were recorded in a range of 15–65°(2 θ). XPS spectra were recorded with an Escalab MK II (VG Company, UK). All binding energies (BE) were calibrated by the BE (284.6 eV) of C1s, which gave BE values within an accuracy of ± 0.1 eV. PL spectra were recorded via a PE LS55 FS spectrometer, with an excitation wavelength of 300 nm. The SPS instrument was assembled at Jilin University, and monochromatic light was obtained by passing light from a 500 W xenon lamp (CHF-XQ500W, China) through a double-prism monochromator (SBP300, China). The slit widths of entrance and exit were 2 and 1 mm, respectively. A lock-in amplifier (SR830, USA), synchronized with a light chopper (SR540, USA), was employed to amplify the photovoltage signal. The powder sample was sandwiched between two ITO glass electrodes.

2.3. Evaluation of the Photocatalytic Activity of Ag-TiO₂. The photocatalytic degradation of RhB on Ag-TiO₂ was carried out in a home-built reactor. A 160 W high-pressure mercury lamp was used as a light source, the intensity of which was 17.1 mW/cm². In each run, 0.15 g of Ag-TiO₂ catalyst was added into 20 mL of RhB solution of 10 mg/L. After the mixture was premixed for 20 min, the light was turned on to initiate the reaction. A HITACHI U-2000 UV-vis spectrometer was used to determine the concentration of RhB solution before and after photocatalytic degradation.

3. Results and Discussion

3.1. XRD Characterization of Ag-TiO₂. Figure 1 shows the XRD patterns of the 5 mol % Ag-TiO₂ powders calcined at different temperatures for 2 h. Figures 2 and 3 show the XRD patterns of Ag-TiO₂ with different doping ratios calcined at 400 °C for 2 and 4 h, respectively. Peaks marked “A” and “R” correspond to anatase and rutile phases, respectively. It can be seen that the phase transformation temperature of TiO₂ in the Ag-TiO₂ catalyst from anatase to rutile went down, and anatase crystallinity was hindered as Ag was doped. The rutile phase began to appear while the Ag-TiO₂ powder was calcined at 500 °C, a considerable amount of anatase transformed into rutile in the powder while the sample was calcined at 600 °C, and all anatase transformed into rutile after calcined at 700 °C. There were two possible reasons for the decrease in the phase

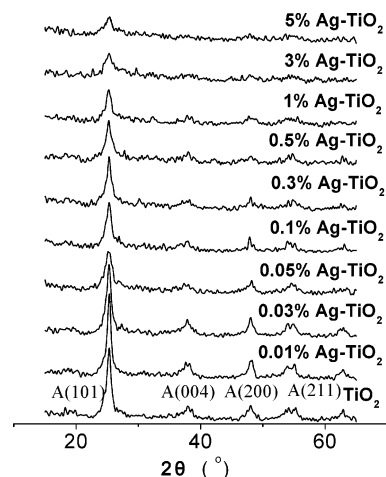


Figure 2. The XRD patterns of Ag-TiO₂ with different doping ratios calcined at 400 °C for 2 h.

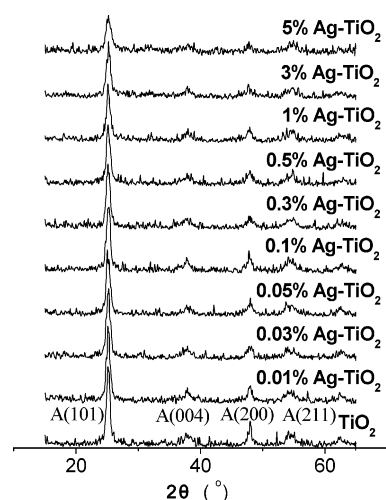


Figure 3. The XRD patterns of Ag-TiO₂ with different doping ratios calcined at 400 °C for 4 h.

transformation temperature. One was that the density of surface defects of Ag-TiO₂ would increase with increasing Ag doping content, which would promote the phase transformation because the surface defects were considered as the rutile nucleation sites.^{12,13} Another was that the surface oxygen vacancy concentration of anatase grains is increased with an increase of the Ag dopant content,¹⁴ which favored the rearrangement of ions and reorganization of structure for rutile phase. Therefore, Ag dopant promoted the anatase to rutile phase transformation. From Figure 1, it can be seen that the Ag crystal phase appeared with an increase in the calcination temperature, indicating that Ag particles were uniformly dispersed on the surface at lower temperature and could aggregate at higher temperature. If the calcination temperature was too low, its crystallinity was imperfect. Thus, too low or high temperature could make the photocatalytic activity decrease. Therefore, an appropriate calcination temperature is needed to obtain an ideal and perfect crystallinity of TiO₂ with Ag dispersed uniformly on its surface. From Figures 2 and 3, we can see that the calcination temperature of 400 °C for 4 h was the appropriate condition for this series of catalysts.

In addition, from the results in Figure 3, it can be seen that the XRD position of TiO₂(101) shifts to low angle with an increase of the Ag dopant content as shown in Table 1. According to Bragg's law, $n\lambda = 2d \sin \theta$, the less is the value of $\sin \theta$, the larger are the d spacings. So, we can conclude that

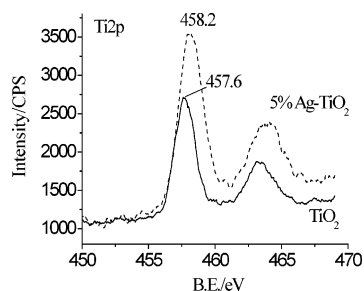


Figure 4. XPS spectra of Ti_{2p} of TiO₂ and 5 mol % Ag–TiO₂.

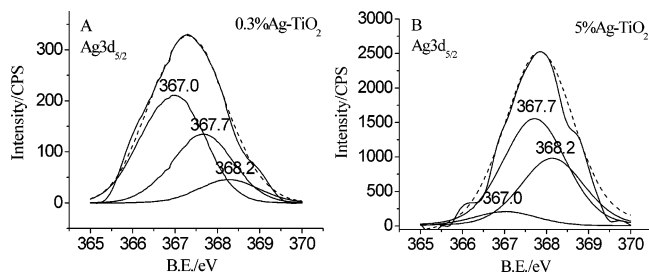


Figure 5. XPS spectra of Ag3d_{5/2} of (A) 0.3 mol % Ag–TiO₂ and (B) 5 mol % Ag–TiO₂.

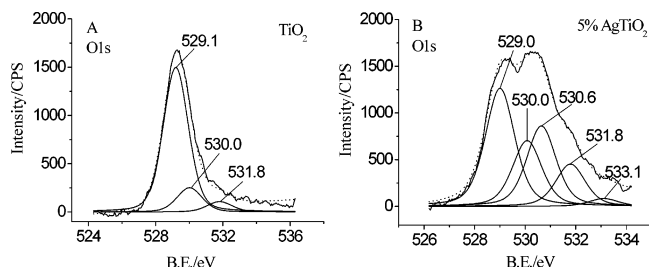


Figure 6. XPS spectra of O1s of (A) TiO₂ and (B) 5 mol % Ag–TiO₂.

TABLE 1: XRD Shift of Different Doping Ratios of Ag–TiO₂

Ag doping ratio (mol %)	0	0.01	0.05	0.5	3
2θ (deg)	25.36	25.32	25.26	25.2	25.06

the value of *d* spacings is gradually increased with an increase in the Ag dopant content. This implies that silver ions diffused into the lattice of TiO₂.

3.2. XPS Measurements. As shown in Figure 4, the Ti_{2p} binding energy of the 5 mol % Ag–TiO₂ sample is increased as compared to that of pure TiO₂. This is because the Fermi level of Ag is lower than that of TiO₂ so that the conduction band electrons of TiO₂ may transfer to the Ag deposited on the surface of TiO₂, which results in a decrease in the outer electron cloud density of Ti ions.

The XPS spectra of Ag3d_{5/2} of the 0.3 mol % Ag–TiO₂ (Figure 5A) and the 5 mol % Ag–TiO₂ (Figure 5B) were fitted with a nonlinear least-squares fit program using Gauss–Lorentzian peak shapes. The XPS spectra of Ag3d_{5/2} indicate that there are three components after deconvolution, attributed to AgO (367.0 eV), Ag₂O (367.7 eV), and Ag⁰ (368.2 eV), respectively.¹⁵ Figure 5 shows that at low concentrations, Ag species mainly exist as AgO and Ag₂O, while at high concentrations, Ag ions and Ag⁰ coexist on the surface, but the amount of Ag⁰ species on the surface is increased remarkably.

The XPS spectra of O1s of the pure TiO₂ (Figure 6A) and the 5 mol % Ag–TiO₂ (Figure 6B) were also fitted with the nonlinear least-squares fit program using Gauss–Lorentzian peak shapes, and three O1s peaks appear after deconvolution, which are attributed to lattice oxygen (529.0 eV), surface

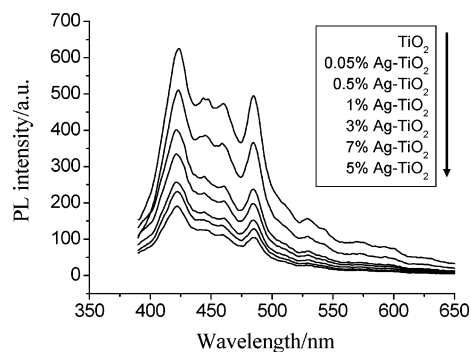


Figure 7. PL spectra of TiO₂ with different Ag doping molar ratios: λ_{Ex} = 300 nm.

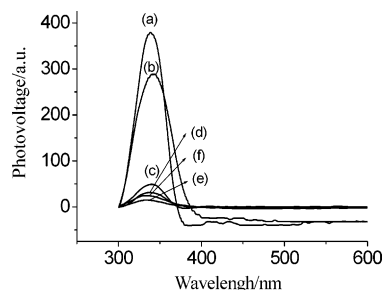


Figure 8. SPS spectra of (a) pure TiO₂ and Ag–TiO₂ with (b) 0.5 mol %, (c) 1 mol %, (d) 3 mol %, (e) 5 mol %, and (f) 7% mol % Ag, respectively.

bridging oxygen (530.0 eV), and surface hydroxyl oxygen (531.8 eV) in TiO₂.¹⁶ Besides, two peaks of O1s originate from Ag–O (530.6 eV) and adsorbed O₂ (533.1 eV), respectively.¹⁵ On the basis of the data of Figure 6, we can conclude that the content of adsorbed O₂ and surface hydroxyl on the surface of Ag–TiO₂ is increased remarkably in contrast to that of pure TiO₂, which is attributed to the deposited Ag enhancing the ability to adsorb O₂.¹⁷ From the above discussion, it can be concluded that the surface states of Ag–TiO₂ were multiple due to simultaneous doping and deposition of Ag species.

3.3. PL and SPS Measurements. Optical properties of solid materials are closely related to their microstructure, such as electronic state, defect state, energy level structure, etc.¹⁸ Luminescence at room temperature, which is impossible for bulk semiconductor, is useful for nanostructured semiconductor. For nanostructured materials, the PL spectra are related to the transfer behavior of the photoinduced electrons and holes so that it can reflect the separation and recombination of photoinduced charge carriers; thus it is used to primarily evaluate the recombination rate of charge carriers.¹⁹

The surface photovoltage (SPV) method is a well-established contactless technique for the characterization of semiconductors, which relies on analyzing illumination-induced changes in the surface voltage.^{20,21} For five decades, it has been used as an extensive source of surface and bulk information on various semiconductors and semiconductor interfaces. Many researchers realized that it is a powerful tool for semiconductor surface characterization and is named as “surface photovoltage spectroscopy” (SPS).²² SPS is more sensitive than X-ray photoelectron or Auger spectroscopy, which makes its scope of applications wider.²³

The SPS technique can provide a rapid, nondestructive monitor of the surface properties of semiconductors.²⁴ It can offer important information about semiconductor surface, interface, and bulk properties, including surface band bending, surface and bulk carrier recombination, surface state distribution,

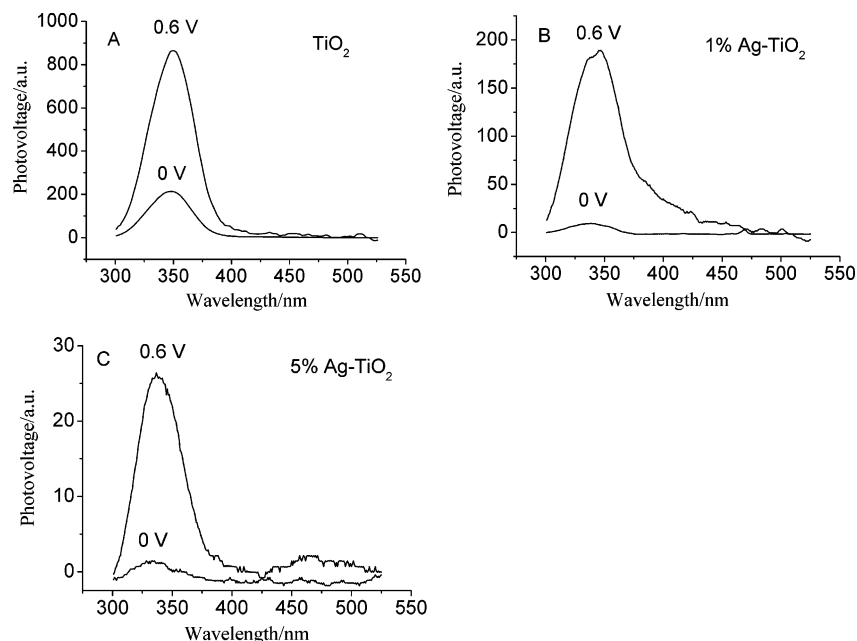


Figure 9. SPS spectra of (A) pure TiO_2 and Ag-TiO_2 with (B) 1 mol %, and (C) 5 mol % Ag with and without a 0.6 V external electric field.

etc., mainly reflecting the carrier separation and transfer behavior with the aid of light,²⁰ especially when the SPS technique is combined with the electric-field-modified technique.²⁵ Hence, the SPS technique is important to semiconductor photocatalysis; that is, SPS measurements can be an effective method for quickly evaluating the photocatalytic activity of semiconductor materials in that it provides a very effective way to study the surface properties involving the charge separation and transfer behavior at the surface or interface as well as the optical characteristics of semiconductor under illumination.²³

As shown in Figures 7 and 8, the PL and SPS intensities are decreased with an increase of the Ag dopant content, and the intensity of the 5% Ag-TiO_2 is lower due to that Ag ions diffused into the crystal lattice of TiO_2 and Ag^0 deposited on the surface can act as traps to capture the photoinduced electron, inhibiting recombination of electron-hole pairs so as to make the SPS response and PL signal decrease. However, when the Ag content exceeds 5%, the Ag^0 particles deposited on the TiO_2 catalyst can aggregate and become larger, resulting in the decrease in the traps of photoelectrons, which lead to an increase in the intensity of the PL and SPS peaks.

Simultaneously doped and deposited Ag with multi-valency state on the superficial layer of TiO_2 can cause the multiple surface states and introduce impurity bands. These surface states and impurity levels play important roles in the photochemical processes to cause sub-band-gap transition, which can take place even illuminated by photons with energy $h\nu < E_g$.²⁰ In general, the transition probability related to the surface states is lower because the transition involving surface states is localized. However, under an appropriate external electric field, this kind of transition can be promoted. The remarkable changes of SPS response of the Ag-TiO_2 nanoparticles can occur in the presence of an external electric field as shown in Figure 9A–C. From Figure 9B, we can see that the SPS signals contain two important regions. One of them at about 350 nm originates from the band–band electron transition of TiO_2 , and the other is a broad SPS response between 400 and 450 nm, which is attributed to the trap-to-band transitions²⁶ caused by the existence of surface oxygen vacancies and hydroxyl. Figure 9C shows a new transition of sub-band-gap at around 470 nm, corresponding to the E_g of about 2.6 eV. The conduction band

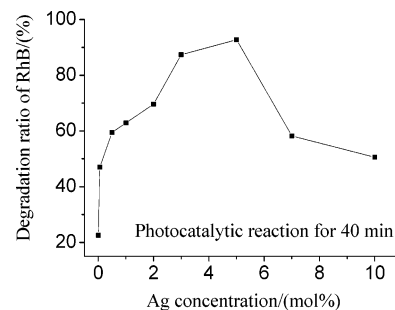


Figure 10. Photocatalytic degradation ratio of RhB over different Ag-TiO_2 photocatalysts.

bottom of Ag_2O ($E_{CB} = 0.34$ V, vs NHE) is 0.64 eV lower than that of TiO_2 . Moreover, the about 2.6 eV needed for the sub-band-gap transition is about 0.6 eV lower than that of the band–band transition. Therefore, it can be concluded that the SPS response at around 470 nm is attributed to the electron transition from the valence band of TiO_2 to the conduction band of Ag_2O .

3.4. Evaluation of Photocatalytic Activity. Figure 10 shows the photocatalytic degradation curves of RhB on Ag-TiO_2 photocatalysts with different Ag dopant content calcined at 400 °C for 4 h. It can be found that the degradation ratio of RhB is increased gradually with an increase in the Ag dopant content. Over 5 mol % Ag-TiO_2 , the degradation ratio is the highest, which could be attributed to the following: (1) The appropriate amount of the doped and deposited Ag species on the surface layer of TiO_2 can effectively capture the photoinduced electrons and holes. (2) Photoinduced electrons can quickly transfer to the oxygen adsorbed on the surface of TiO_2 . (3) The amount of the surface hydroxyl is increased. (4) The response range to light can be expanded to the visible region. These advantages of the Ag-TiO_2 photocatalysts remarkably improve its photocatalytic performance. However, when the Ag content exceeds 5%, the number of active sites capturing the photoinduced electron is decreased with an increase in the size of Ag particles. Moreover, excessive Ag can cover the surface of TiO_2 , leading to a decrease in the concentration of photo-generated charge carrier and photocatalytic activity of photocatalyst. It can be seen that the photocatalytic activity well

corresponds to the intensity of SPS and PL spectra discussed above. This indicates that there is a close relationship between the photocatalytic activity and the intensity of PL and SPS spectra. So, the activity of photocatalyst may be estimated by the PL and SPS measurements.

4. Conclusions

(1) The Ag–TiO₂ has been prepared using a modified sol–gel method in the dark. At rather low Ag dopant concentrations, the migration and diffusion of Ag ions are predominant; AgO and Ag₂O are the main chemical states. While the Ag ions inside the crystal lattice and the surface deposited Ag⁰ coexisted, the amount of the surface deposited Ag⁰ increased remarkably at high dopant concentrations. The Ag–TiO₂ photocatalysts with appropriate content of Ag (Ag species concentration is from about 3 to 5 mol %) possess abundant electronic traps and favor the transfer of the electrons to surface Ag⁰. As a result, the recombination of photoinduced charge carriers can effectively be inhibited. In addition, the content of adsorbed O₂ and surface hydroxyl on the surface of Ag–TiO₂ is increased remarkably in contrast to that of pure TiO₂. These factors can markedly improve the photocatalytic activity of TiO₂.

(2) The photocatalytic experimental results are in good agreement with the conclusions of SPS and PL measurements, indicating that there is a close relationship between the photocatalytic activity and the intensity of PL and SPS spectra. So, the activity of photocatalyst may be estimated by PL and SPS measurements.

(3) The inter-band-gap dopant of Ag₂O can participate in the photochemical processes and extends the absorption of TiO₂ particles into the visible range.

Acknowledgment. This project is supported from the Key Program Projects of National Natural Science Foundation of China (No. 20431030), the National Natural Science Foundation of China (No. 20171016, No. 20301006), the Key Item Project of the Natural Science Foundation of Heilongjiang Province (No. ZJG0404), the Foundation for Excellent Youth of Heilongjiang, the Natural Science Foundation of Heilongjiang Province (No. B0305), and the Science and Technology Project of the

Education Department of Heilongjiang Province (No. 10541171, No. 1054G035), for which we are very grateful.

References and Notes

- (1) Linsebigler, A. L.; Lu, G. Q.; Yates, J. T., Jr. *Chem. Rev.* **1995**, 95, 735.
- (2) Fujishima, A.; Rao, T. N.; Tryk, D. A. *J. Photochem. Photobiol., C* **2000**, 1, 1.
- (3) Grätzel, M. *Curr. Opin. Colloid Interface Sci.* **1999**, 4, 314.
- (4) Bowker, M.; James, D.; Stone, P.; Bennett, R.; Perkins, N.; Millard, L.; Greaves, J.; Dickinson, A. *J. Catal.* **2003**, 217, 427.
- (5) Sano, T.; Kutsuna, S.; Negishi, N.; Takeuchi, K. *J. Mol. Catal. A* **2002**, 189, 263.
- (6) Li, Y. X.; Lu, G.; Li, S. J. *Photochem. Photobiol., A* **2002**, 152, 219.
- (7) Yoon, J. W.; Sasaki, T.; Koshizaki, N.; Enrico, T. *Scr. Mater.* **2001**, 44, 1865.
- (8) Sclafani, A.; Herrmann, J. M. *J. Photochem. Photobiol., A* **1998**, 113, 181.
- (9) Vamathevan, V.; Amal, R.; Beydoun, D.; Low, G.; McEvoy, S. J. *Photochem. Photobiol., A* **2002**, 148, 233.
- (10) Herrmann, J. M.; Disdier, J.; Pichat, P. *J. Catal.* **1988**, 113, 72.
- (11) Kohno, Y.; Hayashi, H.; Takenaka, S.; Tanaka, T.; Funabiki, T.; Yoshida, S. *J. Photochem. Photobiol., A* **1999**, 126, 117.
- (12) Amores, J. M. G.; Escibano, V. S.; Busca, G. *J. Mater. Chem.* **1995**, 5, 1245.
- (13) Amores, J. M. G.; Escibano, V. S.; Busca, G.; Lorenzelli, V. *J. Mater. Chem.* **1994**, 4, 965.
- (14) Chao, H. E.; Yun, Y. U.; Xingfang, H. U.; Larbot, A. *J. Eur. Ceram. Soc.* **2003**, 23, 1457.
- (15) Wagner, C. D.; Riggs, W. M.; Davis, L. E.; Moulder, J. F. *Handbook of X-ray photoelectron spectroscopy*; Perkin-Elmer Corp., Physical Electronics Division: Eden Prairie, MN, 1979.
- (16) Bullock, E. L.; Patthey, L.; Steinemann, S. G. *Surf. Sci.* **1996**, 352–354, 504.
- (17) Cao, X. Z.; Zhang, W. H.; Du, X. G. *Inorganic Chemistry*; High Educ. Press: Beijing, 1994.
- (18) Zhang, L. D.; Mo, C. M. *Nanostruct. Mater.* **1995**, 6, 831.
- (19) Zhu, Y. C.; Ding, C. X. *J. Solid State Chem.* **1999**, 145, 711.
- (20) Kronik, L.; Sapira, Y. *Surf. Sci. Rep.* **1999**, 37, 1.
- (21) Zhai, Q. Z.; Qiu, S. L.; Xiao, F. S.; Zhang, Z. T.; Shao, C. L.; Han, Y. *Mater. Res. Bull.* **2000**, 35, 59.
- (22) Szaro, L.; Rebisz, J.; Misiewicz, J. *Appl. Phys. A* **1999**, 69, 409.
- (23) Jing, L. Q.; Sun, X. J.; Shang, J.; Cai, W. M.; Xu, Z. L.; Du, Y. G.; Fu, H. G. *Sol. Energy Mater. Sol. Cells* **2003**, 79, 133.
- (24) Nauka, K.; Kamins, T. I. *J. Electrochem. Soc.* **1999**, 146, 292.
- (25) Qian, X. M.; Zhang, X. T.; Bai, Y. B.; Li, T. J.; Tang, X. Y.; Wang, E. K.; Dong, S. J. *J. Nanopart. Res.* **2000**, 2, 191.
- (26) Qian, X. M.; Qin, D. Q.; Song, Q.; Bai, Y. B.; Li, T. J.; Tang, X. Y.; Wang, E. K.; Dong, S. J. *Thin Solid Films* **2001**, 385, 152.